The Effect of Vacuum Polarization and Proton Cyclotron Resonances on Photon Propagation in Strongly Magnetized Plasmas

Feryal Özel[1]

Institute for Advanced Study
Einstein Dr., Princeton, NJ 08540; fozel@ias.edu

ABSTRACT

We consider the effects of vacuum polarization and proton cyclotron resonances on the propagation of radiation through a strongly magnetized plasma. We analyze the conditions under which the photons evolve adiabatically through the resonant density and find that the adibaticity condition is satisfied for most photon energies of interest, allowing for a normal-mode treatment of the photon propagation. We then construct radiative equilibrium atmosphere models of strongly magnetized neutron stars that includes these effects, employing a new numerical method that resolves accurately the sharp changes of the absorption and mode-coupling cross sections at the resonant densities. We show that the resulting spectra are modified by both resonances and are harder at all field strengths than a blackbody at the effective temperature. We also show that the narrow absorption features introduced by the proton cyclotron resonance have small equivalent widths. We discuss the implications of our results for properties of thermal emission from the surfaces of young neutron stars.

1. Introduction

Vacuum polarization is a quantum electrodynamical phenomenon that occurs in strong magnetic fields ($B \gtrsim 10^{13}$ G) and affects the interactions between the photons and the electrons. In the presence of a plasma with a density gradient, vacuum polarization gives rise to a resonance when the normal modes of photon propagation change from being mostly circularly polarized at high electron densities to being mostly linearly polarized at low densities. This occurs because, at low plasma densities, virtual pairs of the vacuum dominate the interactions and the photon polarization eigenstates do not correspond to the propagation eigenstates. Thus, at a critical density that depends on photon energy, the conversion of photons between the two polarization modes is highly enhanced, accompanied by a change in the opacities of the normal modes (Adler 1971; Tsai & Erber 1975; Mészáros & Ventura 1979; Kaminker, Pavlov, & Shibanov 1982; see Mészáros 1992 for a review). Another phenomenon that affects the propagation of photons in a magnetized

[1]also Physics Department, Harvard University

plasma is the proton cyclotron resonance that arises from the interaction of the protons in strong magnetic fields with photons. When the field strength is of the order of $B \approx 10^{14} - 10^{15}$ G, the proton cyclotron energy falls in the soft X-ray band and affects the spectral properties of isolated cooling neutron stars.

Because of the sharp transition in the opacities of the normal modes of propagation through the resonances, it has been difficult to include the effects of vacuum polarization in calculations of photon transport in magnetized plasmas. This phenomenon has been treated only recently in the context of interactions of high energy photons with a strongly magnetized plasma by Bezchastnov et al. (1996) and Bulik & Miller (1997) and included in a radiative equilibrium model atmosphere of a neutron star by Özel (2001). It has been shown that the enhanced absorption and mode conversion give rise to broad-band absorption features, which may affect the spectra of high-energy bursts of soft gamma-ray repeaters (Bulik & Miller 1997) and may be responsible for the hard spectral tails observed in the quiescent X-ray emission of radio-quiet neutron stars, such as the anomalous X-ray pulsars (Özel 2001). Proton cyclotron resonance has also been addressed recently in the context of surface emission from strongly magnetized neutron stars (Zane et al. 2001; Ho & Lai 2001). However, a treatment that takes all these effects into account has not yet been developed (see the Appendix for the conceptual and numerical problems with Ho & Lai 2002).

All these radiative transfer calculations involve solving two coupled radiative transfer equations for the two normal modes of propagation. Treating the vacuum polarization resonance in this formalism has some limitations. In particular, the large Faraday depolarization limit assumed in the derivation of the two coupled transfer equation may not hold and an exact treatment may require the solution of four coupled equations for the four Stokes parameters that describe the amplitudes and phases of the electromagnetic waves (see Section 2). However, if the propagation modes evolve adiabatically, the normal mode treatment is valid at densities infinitesimally away from the resonant density and has allowed the derivation of the transfer coefficients in such conditions (Mészáros & Ventura 1979; Pavlov & Shibanov 1979; Kaminker, Pavlov & Shibanov 1982 and references therein). All studies to date involve this treatment, which assumes the adiabatic evolution of the propagation modes and thus includes the enhanced conversion of photons between the two polarization modes near the vacuum polarization resonance. The condition of adibaticity at the resonant density, however, needs to be verified.

In this paper, we first discuss in full generality the propagation of photons in a magnetized plasma in the presence of resonances and determine the conditions under which a normal mode treatment that assumes adiabatic evolution can be employed. We then explicitly show the terms in the radiative transfer equations that describe the enhanced coupling of the photon propagation modes in the presence of vacuum polarization resonance and present a new numerical treatment of the resonances. We also take into account the additional effects of proton cyclotron resonance and present spectra from radiative equilibrium calculations of strongly magnetized neutron star atmospheres when all these effects are taken into account. In an appendix, we address various technical aspects of photon propagation in the presence of a resonance and clarify some incorrect claims that have recently been made in the literature.

2. Adiabatic Evolution of Normal Modes in the Presence of Vacuum Polarization

In this section, we discuss in full generality the propagation of photons through a magnetized plasma when vacuum polarization effects are considered. Our treatment follows closely the discussion in Mészáros (1992, section 6.1d) and Gnedin & Pavlov (1974). We show the derivation of the two coupled equations that describe the transport of radiation in the normal modes, emphasizing the assumptions made in this approach as well as the physical phenomena captured in the resulting equations.

We start by defining the correlation matrix of the components of the electric field of the electromagnetic wave in terms of the four Stokes parameters I, Q, U, and V:

$$\rho_{\alpha\beta} = \frac{1}{2}\begin{pmatrix} I+Q & U+iV \\ U-iV & I-Q \end{pmatrix} \tag{1}$$

so that the the transfer equation that desribes its evolution takes the form

$$(\hat{k}\cdot\vec{\nabla})\rho_{\alpha\beta} = -\frac{1}{2}\sum_{\gamma}(T_{\alpha\gamma}\rho_{\gamma\beta} + \rho_{\alpha\gamma}T^{+}_{\gamma\beta}) + S_{\alpha\beta}. \tag{2}$$

In this equation, $T_{\alpha\beta}$ is the transfer matrix that describes the transition from one polarization to the other as well the absorption and outscattering of radiation, whereas $S_{\alpha\beta}$ is the source matrix that describes emission and inscattering processes. In the basis of eigenvectors of the transfer matrix (which correspond to the normal modes of propagation), the transfer equation becomes

$$(\hat{k}\cdot\vec{\nabla})R_{ij} = -g_{ij}R_{ij} + S_{ij}, \tag{3}$$

where R_{ij} and S_{ij} are the projections of the correlation and source matrices onto the eigenvectors and

$$g_{ij} = \frac{1}{2}(\kappa_i + \kappa_j) + \frac{i\omega}{c}(n_i - n_j). \tag{4}$$

Here, κ_i is the sum of the absorption and scattering coefficients, ω is the photon frequency, and n_i is the refractive index of the ith mode. Note that the two equations for the for the diagonal terms of the correlation matrix R_{ii} correspond to the most general form of equation (14) of Lai & Ho (2002).

When

$$\Im\int_z g_{ij}dz \gg \Re\int_z g_{ij}dz, \tag{5}$$

where $\Im$ and $\Re$ denote the imaginary and real parts of the integral respectively, then the contribution of the non-diagonal terms of g_{ij} to the evolution of R_{ij} is negligible because the integral over this term oscillates rapidly. In this case, the transport of radiation can be described in terms of only two equations for the specific intensity of the two normal modes

$$(\hat{k} \cdot \vec{\nabla}) I_i = -\kappa_i I_i + S_{ii}, \tag{6}$$

i.e., the familiar polarized transfer equations. Here, the term S_{ii}, which takes the form

$$S_{ii} = \sum_j \int d\Omega' \frac{d\sigma_{ij}}{d\Omega} (\Omega' \rightarrow \Omega) I_j(\Omega') \tag{7}$$

when thermal effects are neglected, depends on the specific intensities of both modes and contains information about their coupling through the differential cross section $d\sigma_{ij}/d\Omega$. We will discuss the properties of S_{ii} and specifically the mode coupling in the presence of vacuum polarization resonance in the next section.

In a plasma with gentle density and temperature gradients, the condition (5) becomes

$$\gamma \equiv \frac{\Im \int_z g_{ij} dz}{\Re \int_z g_{ij} dz} = \frac{2\omega(n_i - n_j)}{(\kappa_i - \kappa_j)c} \gg 1, \tag{8}$$

which is generically referred to as the limit of large Faraday depolarization. In all the calculations of photon propagation in magnetized plasmas to date, the normal mode treatment has been employed at the limit of large Faraday depolarization. This requires that the condition (5) holds, i.e., that the propagation modes evolve adiabatically through any density gradient in the plasma, including at the vacuum resonance. In Figure 1, we evaluate the magnitude of the quantity γ to verify the validity of this assumption. We use the model atmosphere calculations discussed in §4 for neutron stars with magnetic fields $B = 5 \times 10^{14}$ G and $B = 10^{15}$ G and effective temperatures $T_{\rm eff} = 0.5$ keV to calculate γ numerically at the resonant density and the corresponding temperature for each photon energy. Note that the quantity γ plotted in this figure includes the effects of both scattering and absorption (see §3 for these expressions; c.f. equation (16) of Lai & Ho 2002).

As Figure 1 shows, the adiabaticity condition holds for photon energies $E \gtrsim 1$ keV for all directions of photon propagation and the magnetic field strengths of interest here, but breaks down at smaller energies. However, the vacuum resonance for these low energies occurs at high optical depths in both modes (see Özel 2001), ensuring that both modes are thermalized and have the same local radiation field density because of high number of interactions. As a result, not including the off-diagonal terms of R_{ij} and g_{ij} in the description of the radiation field at these energies does not affect the results of the transfer calculations.

3. Enhanced Coupling between Normal Modes in the Presence of Vacuum Polarization

Another phenomenon related to the vacuum polarization resonance in strong magnetic fields is the drastic enhancement of the mode-coupling terms in the source matrix $d\sigma_{ij}/d\Omega$, $i \neq j$, which

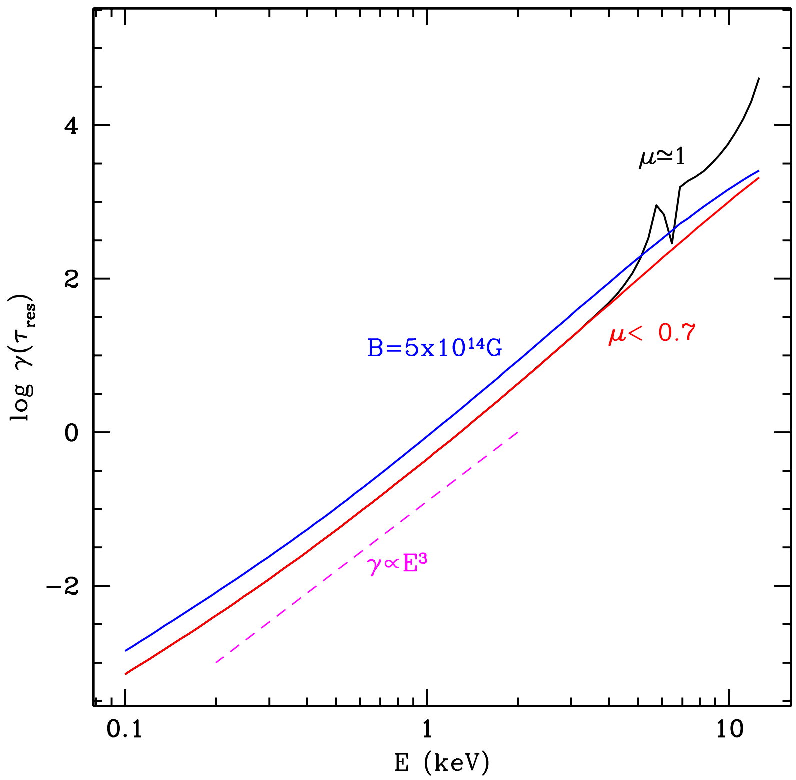

Fig. 1.— The quantity γ that measures the degree of Faraday depolarization at different photon energies, evaluated at the vacuum critical density and the corresponding temperature in a magnetized neutron star atmosphere with $T_{\rm eff} = 0.5$ keV. The two curves labeled with the photon direction of propagation μ correspond to $B = 10^{15}$ G, while the third curve is obtained for $\mu \lesssim 0.7$ at $B = 5 \times 10^{14}$ G. Since $\gamma > 1$ for $E \gtrsim 1$ keV, the adiabaticity condition holds at these photon energies.

describes the redistribution of photons into different directions of propagation and different polarization states. The derivation of the absorption and scattering coefficients κ_i as well as of the matrix $d\sigma_{ij}/d\Omega$, are given in detail in, e.g., Mészáros & Ventura (1979) and Mészáros (1992). The standard procedure involves combining the sourceless Maxwell's equations into a wave equation, casting it in the form of the transfer equation, and identifying the various terms with the elements of the matrices g_{ij} and S_{ij} (eq. [3]). Therefore, these terms take into account *all* the mode-changing processes in a plasma, whether or not they arise from a single scattering or, as discussed in detail in Mészáros (1992, p.97), from non-linear effects near the vacuum resonance (assuming adiabatic mode evolution).

Because we are specifically interested in the off-diagonal, mode-changing terms of the photon redistribution matrix $d\sigma_{ij}/d\Omega$, we highlight two interesting phenomena that have a significant contribution to these terms (see also Ho & Lai 2002). The photons interact with both the electrons and the protons in the plasma. When the field strength is sufficiently high ($B \approx 10^{14-15}$ G), the proton cyclotron energy lies in the keV range and affects the X-ray spectra of magnetized sources. Just like the electron cyclotron resonance, the proton cyclotron resonance gives rise to enhanced mode coupling due to its effect on the normal modes of propagation (see below) and to absorption features in the spectra of photons emerging from magnetized plasmas.

The second and most interesting effect in strong magnetic fields arises from the presence of virtual pairs which change the interaction of the photons with the plasma and thus its index of refraction. This happens through the effect of the virtual pairs on the normal modes of propagation as discussed earlier. The expressions for the absorptive and dispersive properties of the plasma under these conditions were derived by Adler (1971) and Tsai & Erber (1975).

When the plasma electrons and protons as well as the vacuum polarization effects are considered, the parameter that determines the ellipticities of the normal modes of photon propagation take on the form

$$q = \frac{\sin^2\theta}{2\cos\theta}(1-u_p)\sqrt{u}\left(1 - W\frac{u-1}{u^2}\right), \tag{9}$$

where $u = E_b^2/E^2, u_p = E_p^2/E^2, E_b$ is the electron cyclotron energy, E_p is the proton cyclotron energy, and E denotes the photon energy. The vacuum parameter W represents the correction to the index of refraction due to vacuum polarization and has two limiting forms; for $B < B_{\rm cr} = 4.41 \times 10^{14}$ G it is given by

$$W = \frac{\alpha}{15\pi}\left(\frac{B}{B_{\rm cr}}\right)^2\left(\frac{E_{\rm b}}{E_{\rm pl}}\right)^2 = \left(\frac{3\times 10^{28}{\rm cm}^{-3}}{N_e}\right)\left(\frac{B}{B_{cr}}\right)^4. \tag{10}$$

while for $B > B_{\rm cr}$, it can be written as

$$\begin{aligned} W \;=\; & \frac{\alpha}{2\pi}\left[\frac{2}{3}(\frac{B}{B_{\rm cr}}) - 1.27 + \frac{B_{\rm cr}}{B}\ln\left(2\frac{B}{B_{\rm cr}}\right) - 0.386\frac{B_{\rm cr}}{B} + 0.70\left(\frac{B_{\rm cr}}{B}\right)^2\right. \\ & \left. -\frac{2}{3} + \frac{B_{\rm cr}}{B}\ln\left(2\frac{B}{B_{\rm cr}}\right) - 0.838\frac{B_{\rm cr}}{B} + \left(\frac{B_{\rm cr}}{B}\right)^2\right]\left(\frac{E_{\rm b}}{E_{\rm pl}}\right)^2, \end{aligned} \tag{11}$$

where we used the expansions of the electromagnetic Lagrangian given in Tsai & Erber (1975, Eq. 38a-b). In these expressions, α is the fine-structure constant, $E_{\rm pl}$ is the plasma frequency and N_e is the electron density. Given the ellipticities of the normal modes of propagation, it is straightforward to calculate the absorption and scattering terms in equation (6).

The quantity q determines directly the polarizations of the normal modes and thus all the elements of $d\sigma_{ij}/d\Omega$, which involve the moduli of the cyclic projections of the unit polarization vectors onto the coordinate axis with a given magnetic field direction. In Figure 2, we plot the off-diagonal terms of $d\sigma_{ij}/d\Omega$ as a function of electron density for different photon energies and directions of propagation.

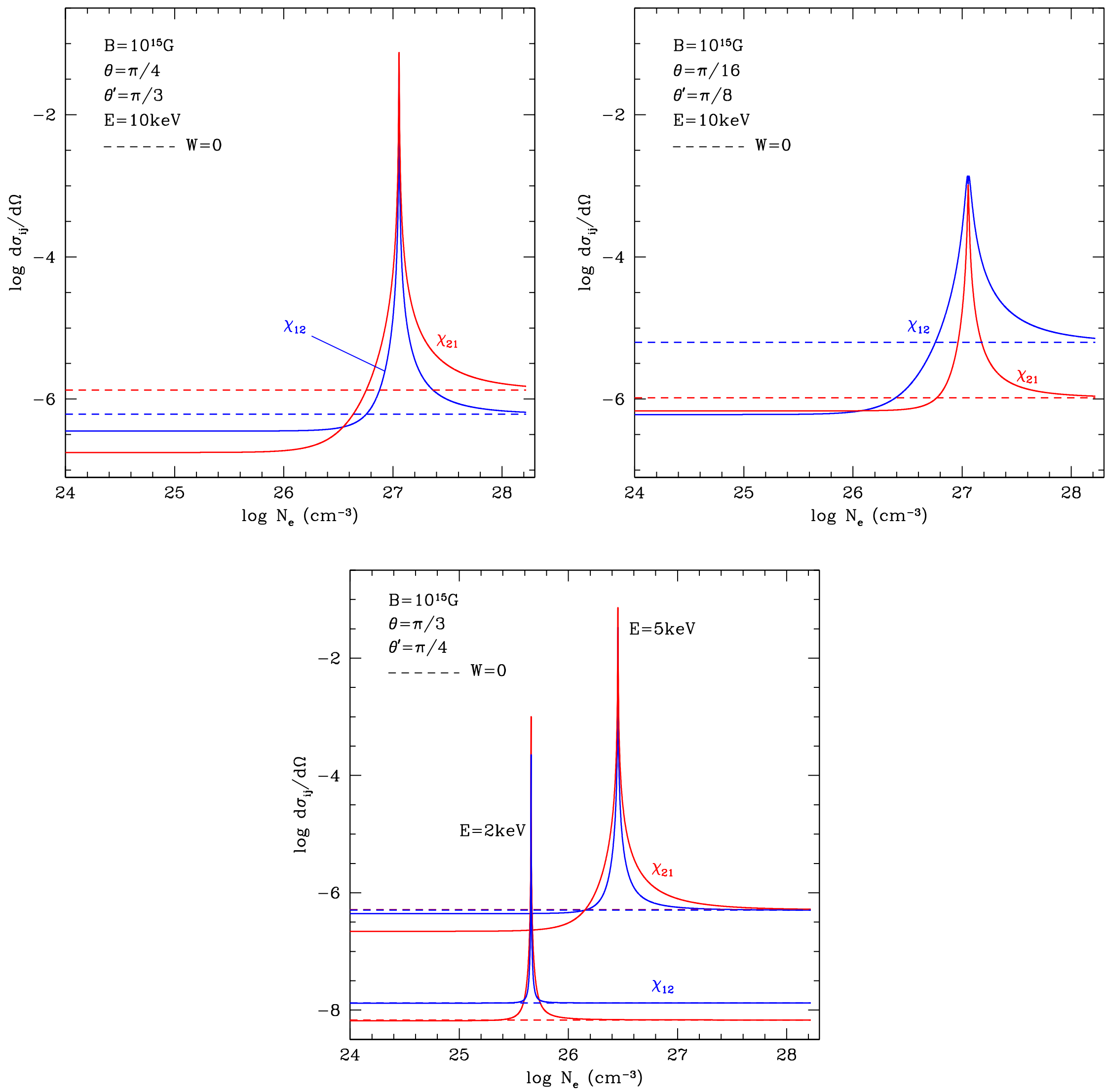

Fig. 2.— The off-diagonal, mode-coupling terms of the scattering matrix $d\sigma_{ij}/d\Omega$, in units of $N_e\sigma_{\rm T}$, as a function of particle density in the atmosphere. In all the panels, solid lines show the terms when vacuum effects are included and the dashed lines when these effects are neglected. Coupling of photons with different directions of propagation and different energies are shown in panels (b) and (c), respectively.

Figure 2 shows a remarkable enhancement in the off-diagonal terms of the scattering matrix near the vacuum resonance density. These terms describe *true* propagation-mode changing and can significantly alter the spectrum and angular distribution of radiation propagating through a magnetized medium. This is because they can convert a photon from a mode with a small mean-free path to one with a large mean-free path and vice versa. As the different panels of Figure 2 show, the conversion probability and the width of the resonance depends on the photon energy and direction of propagation.

These rapidly-changing off-diagonal terms are difficult to handle numerically when modeling the transport of radiation. A number of different approaches have been employed to date, which we discuss in the next section.

4. Numerical Treatments of the Resonance and Mode Coupling

As discussed in §3, vacuum polarization introduces narrow and energy-dependent resonances in the opacities and cross-mode interaction terms. Given that the radiative equilibrium calculations require an energy grid that extends over four orders of magnitude and a depth grid that spans ten orders of magnitude, resolving the resonance by using an arbitrarily large number of grid points in these two variables is computationally prohibitive. Instead, the solution requires new numerical methods, which can sample the resonance region with high accuracy. The accuracy of the solutions depends on a correct calculation of the total optical depth under the resonance.

Here we introduce a new algorithm to overcome this problem that involves sampling the resonance region with a very large number of points on an auxiliary grid (denoted by prime) in order to compute accurately the total optical depth. We smooth the redistribution matrix elements according to

$$\frac{d\sigma_{ij}^{\rm n}}{d\Omega}(\tau_{\rm es}) = \int \frac{d\sigma_{ij}}{d\Omega}(\tau_{\rm es}')\frac{1}{\sqrt{2\pi\sigma^2}} \exp\frac{-(\tau_{\rm es}-\tau_{\rm es}')^2}{2\sigma^2} d\tau_{\rm es}' \tag{12}$$

where $d\sigma_{ij}^{\rm n}/d\Omega$ denotes the new smoothed matrix elements and the smoothing factor σ in the Gaussian is chosen based on the number of points in the main depth grid. The number of points on the auxiliary grid can be arbitrarily large without increasing significantly the computational time. (Note that we also compute the absorption coefficients in this way). This method allows the sharp features to be resolved on the discrete grid while preserving the total optical depth across the resonance. As a result, it yields the most accurate solution allowed for a chosen number of grid points, as well as smooth spectra. In the calculations presented in §4, we employ a depth grid of 400 and an energy grid of 80 points.

4.1. Comparison with Previous Methods

We now compare the above algorithm to the numerical methods have been developed earlier to treat the transfer of radiation through the vacuum polarization resonance.

Monte Carlo Methods.— Bulik & Miller (1997) used a Monte Carlo technique to follow the propagation of photons through a hot, ultramagnetized plasma. Since Monte Carlo methods are not grid-based but follow the trajectories of individual photons, they have little difficulty in handling

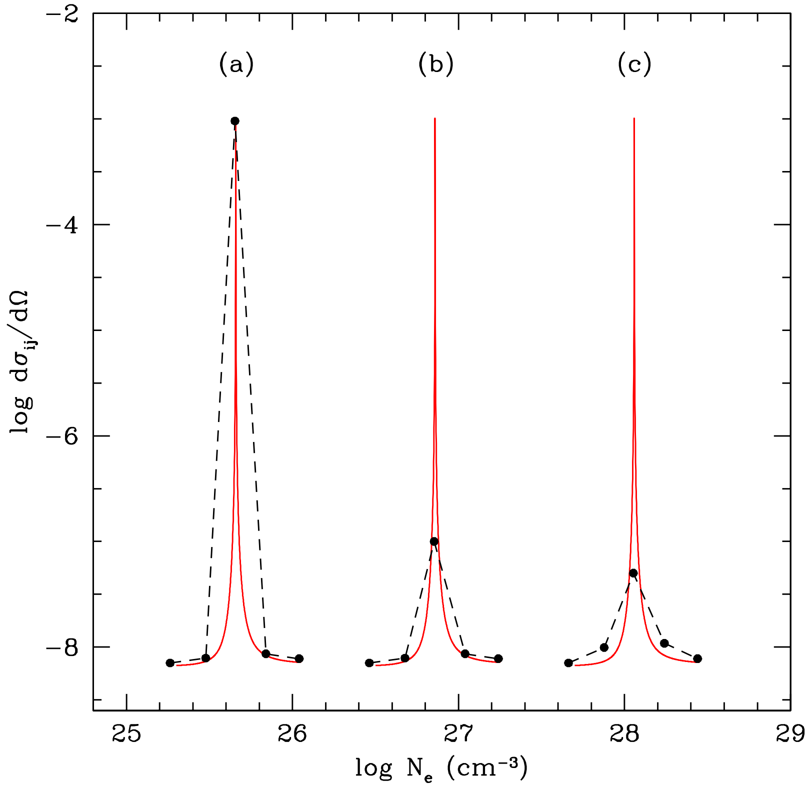

Fig. 3.— A schematic representation of three different grid choices for resolving a vacuum resonance feature: (a) the equal-grid method of Ho & Lai (2002), (b) the saturation method of Özel (2001), and (c) the Gaussian-smoothing method presented here.

the sharp vacuum resonances. They also allow an easy implementation of non-coherent (Compton) scattering, which was important for the high temperature plasmas considered by Bulik & Miller (1997). This method, however, suffers from small number statistics that produces numerical noise in the calculated spectra. It is also not suitable for steady-state calculations in which the radiative equilibrium condition is required throughout the medium, as in the case of a cooling neutron star atmosphere.

Grid-based Methods.— Grid-based methods facilitate the construction of atmosphere models in steady-state in which the radiative equilibrium condition is imposed. Such methods are not constrained by small number statistics and can resolve sharp features given a carefully chosen grid. In the presence of vacuum polarization and cyclotron resonances, the choice of grid is crucial in capturing the effects discussed in §3. A typical resonance in the off-diagonal terms of the scattering matrix is illustrated in Figure 3, along with three different choices of grid that have been recently employed.

Ho & Lai (2002) used a scheme, the equal-grid method, in which for every energy grid point, the vacuum resonant density corresponds to a depth grid point (Fig. 3, case a). This choice ensures a uniform sampling of all resonant features and thus the smoothness of the resulting spectra. However, because the vacuum features are very narrow, such a choice always overestimates significantly the total optical depth across the resonance as is evident in the figure. Indeed, even though the calculated spectra are smooth, they have artificial "absorption-like" features that are reduced as the number of grid points increases (see Fig. 9 of Ho & Lai 2002). Note, however, that even at the highest number of grid points used by Ho & Lai (2002), the artificial features are still present in the spectra which have not approached the true solution. It is likely that this effect is also responsible for the discrepancy at low energies between the "no-conversion" and "mode-conversion" solutions presented in Figures 11 and 12 of Ho & Lai (2002).

Özel (2001) approached this problem by devising a saturation scheme which truncates the sharp resonant features (Fig.3, case b). In this method, a large number of grid points in column depth are used to ensure that for every energy, at least one depth grid point samples the saturated value of the resonant feature. This method underestimates the optical depth across the resonance but, for the same number of grid points, the error introduced is much smaller than the equal grid method (see Fig. 3). It also converges faster to the true solution as the number of grid points increases. Note that in Özel (2001), a saturation value and the corresponding number of grid points were chosen such that the solutions reached an asymptotic limit and did not depend on the particular choices.

Note, however, that the computed optical depth under the vacuum feature, which determines the accuracy of the solutions, in not preserved in either method discussed above. This is contrast to the new method presented in this paper, which is shown as case (c) in Figure 3.

Finally, the "step-function" method involves matching and exchanging the opacities of the two polarization modes below and above the resonance without resolving the transition region. It was first introduced by Zane et al. (2001) in the case of ultramagnetized neutron star atmospheres and is also used in Ho & Lai (2002) in their "complete mode conversion" calculations. This approximate method is highly inaccurate and provides no advantages over the equal-grid method in resolving the sharp change of the absorption coefficients near the resonance as it equally misestimates the total optical depth across the resonance.

5. The Effect of Vacuum Polarization and Proton Cyclotron Resonances on Radiation Spectra

We now discuss the effect of the vacuum polarization and proton cyclotron resonances on the spectra of emission from the surface of a strongly magnetized neutron star. Computing the spectrum of surface radiation requires the solution of the two coupled equations that describe the propagation of the photons through the magnetized plasma, subject to the condition of radiative

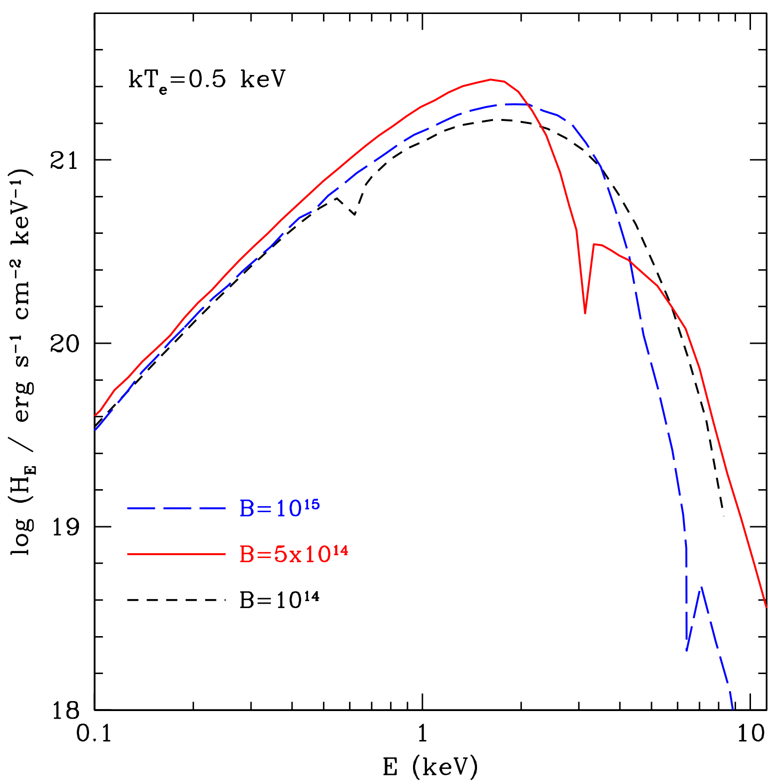

Fig. 4.— The spectra of radiation emerging from a strongly magnetized neutron star atmosphere of $T_e = 0.5$ keV, when proton cyclotron and vacuum resonances have been taken into account.

equilibrium in a hydrostatic atmosphere. In the calculations presented here, we follow the methods described in Özel (2001) with the addition of the new algorithm for handling resonances discussed in the previous section. Briefly, we use a modified Feautrier method for the solution of the angle- and polarization-mode dependent radiative transfer problem and ensure radiative equilibrium with a temperature correction scheme based on the Lucy-Unsöld algorithm. The implementations of these methods are given in Özel (2001).

Figure 4 shows the spectra of surface emission from a neutron star with $B = 10^{14} - 10^{15}$ G and with an effective temperature of $T_{\rm e} = 0.5$ keV. The spectra at all field strengths are harder than a blackbody at $T_{\rm e} = 0.5$ keV. However, the shape of the continuum as well as the narrow features that appear due to the proton cyclotron resonance depend strongly on the magnetic field.

The shape of the continuum is determined by both the vacuum polarization and the proton cyclotron resonances. As discussed in Özel (2001), the vacuum resonance introduces a layer of enhanced interactions and brings the thermalization depth of all photons with $E \gtrsim 2$ keV closer to the outermost layers of the atmosphere. The sudden increase in the opacity at these photon-energy dependent critical densities leads to broad-band absorption-like features in the spectrum. However, because this resonance has a strong dependence on photon energy that causes less attenuation of the flux at higher photon energies, it leads to a hardening of the spectrum at $E \gtrsim 2$ keV for $B \gtrsim 10^{14}$ G as well as to increased flux at photon energies $E \lesssim 1$ keV, as discussed in Özel (2001) and Bulik & Miller (1997). Note that the resonance does not soften the spectrum but indeed is *responsible* for the hard tails at $E > 2$ keV.

The spectra in Figure 4, however, do not all show these hard tails because the proton cyclotron resonance also affects the shape of the continuum through its modification of the ellipticities of the normal modes and its contribution to the opacities. In particular, it gives rise to a broad absorption feature that reduces the continuum flux around the proton cyclotron energy for $B \gtrsim$ few $\times 10^{14}$ G. For $B \sim 5 \times 10^{14}$ G, the cyclotron absorption modifies the peak of the spectrum, leading to a sharper fall-off at $E \sim 2$ keV, while for $B \sim 10^{15}$ G, it suppresses the spectral tail in the $5-10$ keV energy range.

The narrow features at the proton cyclotron energy, on the other hand, arise from the enhanced interaction of the protons with the photons at that energy. These features are weak in the presence of the vacuum polarization resonance: the thermalization depth of the photons in nearby energies are brought closer to the thermalization depth at the cyclotron energy because of the vacuum polarization resonance, thus reducing the contrast between the flux at these photon energies. The resulting features have small equivalent widths at all field strengths considered here: at $B = 5 \times 10^{14}$ G, the equivalent width is ~ 80 eV, while at $B = 10^{15}$ G, the equivalent width is ~ 0.2 keV. These features are likely to have even smaller equivalent widths as seen by an observer at infinity because of the effects of phase averaging and redshifts on the observed spectra.

6. Conclusions

In this paper, we have considered the various effects of vacuum polarization and proton cyclotron resonances on the propagation of photons through a strongly magnetized plasma. Given that the treatment of photon transport by solving two coupled transfer equations for two normal modes of propagation assumes large Faraday depolarization, we have first checked whether this condition is satisfied at the resonant densities for all photon energies. We have found that for photon energies $E \gtrsim 1$ keV, the assumption is satisfied, i.e., the modes evolve adiabatically through the resonance, for all directions of propagation at the magnetic field strengths considered here. The resonant layer for photons with smaller energies lies deeper in the atmosphere than their thermalization depths and thus does not affect their propagation. Employing a normal mode treatment to calculate the properties of radiation emerging from a magnetized plasma is therefore justified.

We have then constructed radiative equilibrium atmosphere models of strongly magnetized neutron stars that includes the effects of vacuum polarization and proton cyclotron resonances. We have introduced a new numerical method that resolves accurately the sharp changes of the absorption and mode-coupling cross sections at the resonant densities. In particular, this method involves sampling the resonance region with a very large number of points on an auxiliary grid and thus allows for an accurate computation of the total optical depth across the resonances. Using this method in addition to those described in Özel (2001) for the solution of the transfer problem subject to the radiative equilibrium condition, we have calculated the spectral energy distributions of a cooling neutron star atmosphere.

We have shown that the resulting spectra are harder at all magnetic field strengths than a blackbody at the effective temperature but the shape of the continuum depends strongly on the field strength, shaped by the broad-band absorption due to both resonances. In particular, the suppression of the flux due to the proton cyclotron resonance dramatically reduces the hard tails at $E > 3$ keV that arise from the vacuum resonance at $B = 10^{15}$ G. In contrast, it only modifies the peak of the spectrum at $B = 5 \times 10^{14}$ G and, together with the vacuum resonance, gives rise to a hard tail of photon index $\Gamma \approx 2 - 3$ in the $2 - 6$ keV range. Note that hard tails have been observed in this energy range in a number of sources that are currently the best candidates for being ultramagnetized neutron stars, such as the anomalous X-ray pulsars and soft gamma-ray repeaters. However, a conclusive statement can be made by comparing the observations of these sources to spectral models that take into account the effects of the gravitational redshift and phase-averaging.

Finally, we have shown that the narrow absorption features introduced by the proton cyclotron resonance have small equivalent widths. The vacuum polarization resonance significantly suppresses the strengths of these lines by bringing the thermalization depth of photons that have energies in the vicinity of the cyclotron energy further out in the atmosphere and thus closer to that of the photons at the cyclotron energy. These small equivalent widths may help explain the lack of narrow absorption features in the observations of anomalous X-ray pulsars and soft gamma-ray repeaters (Juett et al. 2001; Patel et al. 2001). Deeper observations of these sources, especially with instruments that have higher sensitivity at $E \gtrsim 5$ keV range may help reveal some of these features and thus the nature of these intriguing objects.

I thank John Bahcall for his valuable input and discussions on the physics of mode evolution across resonances. I also thank Dimitrios Psaltis for many discussions on the treatment of resonances in radiative transfer problems and Ramesh Narayan for useful suggestions. This work was supported in part by a fellowship of the Keck Foundation and an NSF grant PHY-0070928.

A. On the Adiabatic Mode Evolution and Mode Conversion near the Vacuum Polarization Resonance

In a recent paper, Lai & Ho (2002) discussed the physics of vacuum polarization resonance and pointed out the well-known effects of adiabatic evolution and enhanced polarization mode conversion that take place through the resonant density (see the references in §1). They argued that this effect was not treated in previous studies and evaluated the conditions under which the large Faraday depolarization assumption and hence the adiabatic evolution of modes breaks down. In a subsequent work, Ho & Lai (2002) further claimed that they included for the first time the effect of this new phenomenon on the spectra of a magnetized neutron star atmosphere in radiative equilibrium.

In this appendix, we clarify the effects of vacuum polarization resonance on the normal-mode description of photon transport in magnetized media. We show that the effects discussed by Lai & Ho (2002) have been taken into account in the previous calculations of photon transport through a plasma (Bulik & Miller 1997; Zane et al. 2000; Özel 2001). In particular, as long as a normal-mode treatment is employed, the physics included in the calculations is the same, independent of the nomenclature with which one describes modes above and below the resonant density. Below, we outline some of the mistakes and inconsistencies in their discussion.

First, referring to the case where the photon modes evolve adiabatically as "mode conversion" is misleading, since this is precisely the case where the normal modes of propagation ($i = 1, 2$ or $-/+$ modes) remains the same above and below the resonance. What *is* different is the correspondence between the polarization and propagation eigenstates on the two sides of the resonance. Note in particular that equations (2.27) and (2.43) of Ho & Lai (2002), which presumably describe the two different definitions of normal modes, are mathematically identical.

Second, adiabatic evolution is not an additional effect that needs to be *included* in calculations of radiative transport; it is by definition part of the calculations. In fact, as we discussed in §2, solving the transfer equation in the two normal modes *requires* that the modes evolve adiabatically. What the modes are called above and below the resonant density is irrelevant, given that the transfer equations are written for the normal modes of propagation and not for polarization eigenstates (the so-called extraordinary and ordinary modes) as we discussed above. Therefore, they criticise incorrectly the previous works for not including this new physical effect. For the same reasons, it is in fact meaningless to "include" or to "neglect" mode conversion (in the terminology of Lai & Ho 2002) because neglecting the adiabatic mode evolution does not describe any physical situation. The difference in the results between these two cases most likely arises from the different numerical treatments the authors employ in each case, both of which are highly inaccurate as discussed in §4.

Ho & Lai (2002, §2.4) also claim that in the limit of non-adibaticity, the radiative transfer formalism breaks down and cannot describe the evolution of photons. This is also incorrect. As discussed above, one simply needs to solve all four equations (3) in this case rather than the two equations for the diagonal terms of R_{ij}. We emphasize that this case is not relevant for the problem discussed here but in general can be easily addressed by keeping the equations for the off-diagonal terms.

REFERENCES

Adler, S. L. 1971, Ann. Phys., 67, 599

Bezchastnov, V. G., Pavlov, G. G., Shibanov, Y. A., & Zavlin, V. E. 1996, Gamma-Ray Bursts, Proceedings of the 3rd Huntsville Symposium (Woodbury, AIP) eds. C. Kouveliotou, M. F. Briggs, and G. J. Fishman, 907

Bulik, T. & Miller, M. C. 1997, MNRAS, 288, 596

Gnedin, I. N. & Pavlov, G. G. 1974, Zhurnal Eksperimental noi i Teoreticheskoi Fiziki, 65, 1806

Ho, W. C. G. & Lai, D. 2001, MNRAS, 327, 1081

Ho, W. C. G. & Lai, D. 2002, MNRAS, submitted (astro-ph/0201380)

Juett, A. M., Marshall, H. L., Chakrabarty, D., & Schulz, N. S. 2002, ApJ, 568, L31

Kaminker, A. D., Pavlov, G. G., & Shibanov, I. A. 1982, Ap&SS, 86, 249

Lai, D. & Ho, W. C. G. 2002, ApJ, 566, 373

Mészáros, P. 1992, High-Energy Radiation from Magnetized Neutron Stars (Chicago: University Press)

Meszaros, P. & Ventura, J. 1979, Phys. Rev. D, 19, 3565

Özel, F. 2001, ApJ, 563, 276

Patel, S. K. et al. 2001, ApJ, 563, L45

Pavlov, G. G. & Shibanov, I. A. 1978, Sov. Astr., 22, 214

———. 1979, Sov. Phys. JETP, 49, 741

Tsai, W. & Erber, T. 1975, Phys. Rev. D, 12, 1132

Zane, S., Turolla, R., Stella, L., & Treves, A. 2001, ApJ, 560

AAS LaTeX macros v5.0.